Aerial Display of Vibrotactile Sensation with High Spatial-Temporal Resolution using Large-Aperture Airborne Ultrasound Phased Array

Keisuke Hasegawa   Hiroyuki Shinoda

Graduate School of Information Science and Technology, the University of Tokyo

ABSTRACT

We fabricated a tactile display which can generate vibrotactile sensation on human skin on which no equipment is mounted. It utilizes focused airborne ultrasound radiation pressure for stimulation. The workspace of our new tactile display is widened to a cube of 1m x 1m x 1m, which allows users free motions in it. In order to widen the workspace, our new prototype integrates multiple ultrasound transducer units and achieves a large aperture airborne ultrasound phased array. As the workspace is widened, it has become possible to stimulate arbitrary regions all over a human body.

The amplitude of imposed radiation pressure can be time-variant. The profiles of generated vibrotactile stimuli can be designed with a temporal resolution of 0.5 ms and 320-level quantization of radiation pressure amplitude. It is easy to choose a recorded waveform and reproduce it as vibrotactile stimuli at an arbitrary spatial point. This paper introduces how our new tactile display works and reports its performance evaluation.

KEYWORDS: Airborne Ultrasound, Vibrotactile Sensation, Whole-body Passive Tactile Display

INDEX TERMS: [Communication hardware, interfaces and storage]: Tactile and hand-based interfaces—Haptic Devices; [Human computer interaction (HCI)]: Interaction Devices—Haptic Devices

1   INTRODUCTION

Tactile displays have been of interests among researchers and a great variety of devices have been developed. In general, the time-variant component in tactile sensation is considered to be important for human in determining various tactile textures. The four types of major mechanoreceptors are well known for their coherent time-space characteristics and their contribution to tactile information transmission has also been widely investigated. This temporally characterized tactile sensation is in particular called vibrotactile sensation and many researches of tactile information display focus on representation of it [1][2].

Most of the current vibrotactile devices need to be mounted or held on human bodies. It means that only surfaces of human bodies in contact with the device can receive vibrotactile stimuli. In addition, free movement of users may be constrained by the mounted devices. In a few attempts to generate noncontact tactile sensation by using air jet [3], the workspace is still constrained within the near field of the jet nozzle and the design freedom in temporal profile of stimulation seems limited. There have been wearable vibrotactile displays e.g. [4], nevertheless, to the best of our knowledge, a system which can remotely stimulate from top to toe has not been developed yet. In public use or applications for
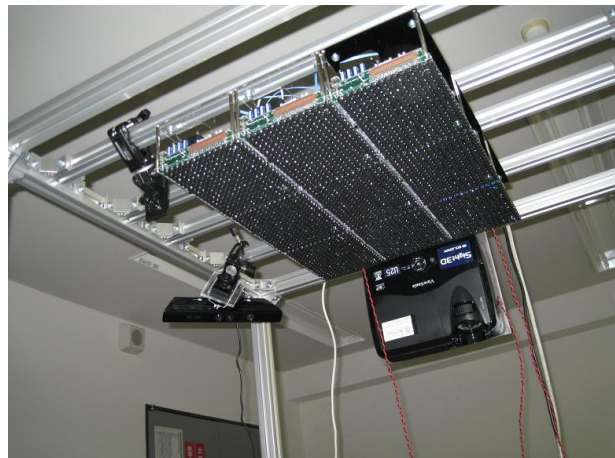
Figure 1: Our newest system of the 9-unit AUTD. The total area of the 3 by 3 units is 57×45cm^2.

alarming, the requirement of wearing some special devices in advance can be a crucial problem.

If we can construct a system which generates tactile sensations in arbitrary positions all over our bodies without constraining our body movement, the range of possible applications will be greatly broadened. For example, it will be possible to tactually give users caution wherever they are. Since they do not need to possess any devices, unspecified number of users there will be able to receive tactile information. In this example, users feel tactile sensation on unexpected and unintended timing. "Passive touch" sensation like this brings much richer experience in virtual reality applications. We can explore in jungles, as shoving branches and grasses with our arms and legs. Sometimes creatures like bugs or frogs may jump into our faces. These experiences will be much more realistic when proper tactile stimulation is added to the visual and audible contents. For this purpose, tactile sensations must be conveyed without constraining users' movement in situations like this.

We have been investigating the Airborne Ultrasound Tactile Display (AUTD) [5][6], which exploits focused airborne ultrasound on human skin to generate vibrotactile sensations. AUTD can generate vibrotactile sensations in any positions in the air. Since AUTD utilizes propagating ultrasound, the temporal profile of output waveform is mostly preserved through distance. This property of sound propagation enables to convey complicated vibration on human skin remotely. By switching the focal position quickly, multiple users can receive tactile sensation simultaneously. Temporal profiles of vibrotactile stimuli by AUTD are programmable and are even possible to be generated from recorded vibration signals. As recent researches show [7], reproducing vibrations faithfully can display realistic tactile feeling.

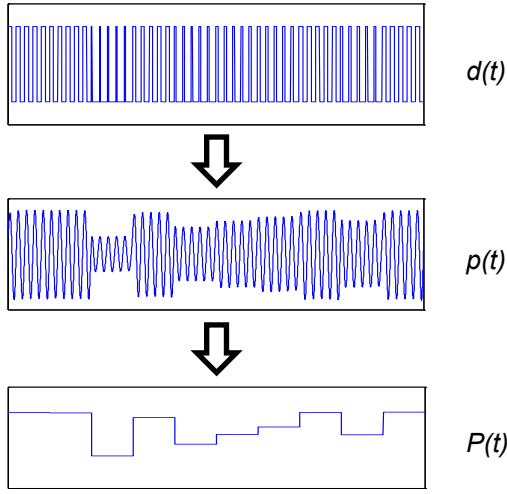In this paper we describe the principle of our newly fabricated

Figure 2: Diagram of driving pulse signals $d(t)$, sound pressures $p(t)$ and radiation pressures $P(t)$.

system (Figure 1) and some experimental results of its performance evaluation. As a result, we succeeded in generating focused ultrasound as tactile stimuli on human skin 600 mm apart from the new tactile display of a 576 mm x 454.2 mm aperture. The focal intensity was 7.4 gf. We also designed temporal profiles of generated vibrotactile stimulation with a temporal resolution of 0.5 ms and 320-level quantization. We observed the radiation pressure and it was consistent with the designed profiles. We performed a human study, where the subjects were asked to identify the temporal profiles of vibrotactile stimuli displayed by the system among four different patterns. As a consequence, it was proven that some of the temporal profiles were distinguishable for the subjects.

2 PRINCIPLE OF REMOTE VIBROTACTILE SENSATION PRODUCTION USING AIRBORNE ULTRASOUND

The proposed system produces vibrotactile stimulation on human skin via air using focused ultrasound. We make use of the acoustic radiation pressure, which is a nonlinear acoustic phenomenon, to convert the alternating sound pressure amplitude into static pressure to deform skin surfaces. This radiation pressure can be focused in an arbitrary position by choosing the phase shift of each transducer appropriately. A temporal profile of radiation pressure is manipulated by changing the pulse-wise modulation duty cycles of ultrasound transducers. Based on these schemes, our system can produce various profiles of vibrotactile sensation in arbitrary position all over our bodies.

2.1 Acoustic Radiation Pressure

The acoustic radiation pressure is a nonlinear phenomenon of sound propagation [8]. When the amplitude of sound source becomes high (typically 120 dB~), the propagating waveform is highly distorted and biased. As a result, the time average of the waveform becomes non-zero. This yields static pressure on the surface of an object when it blocks off the wave propagation. This pressure is called acoustic radiation pressure and its value P [Pa] is estimated as

$$P = \frac{\alpha p^2}{\rho c^2},\qquad(1)$$

where p[Pa] denotes the sound amplitude, c[m/s] denotes the

sound velocity in the medium, ρ[kg/m^3] denotes the density of the medium and α denotes the coherent coefficient determined by the acoustic impedance of the medium and the object to block off the ultrasound propagation. When ultrasound propagates in the air and blocked off by liquid or solid, almost all of the ultrasound is reflected on the boundary and in this case the coefficient α becomes nearly 2. Here p is the instantaneous RMS of the sound amplitude. Therefore if the ultrasound frequency is high enough compared to the time variation of p, the outcome radiation pressure P varies temporally as p does. Thus we can control temporal profiles of radiation pressure by controlling the envelope of ultrasound pressure. The attenuation of ultrasound propagation depends on its frequency. The attenuation rate of 40 kHz ultrasound in air is about 1 dB/m. This frequency is much higher than the highest frequency that human can feel as vibrotactile stimulation (~1 kHz) [9]. From these specifications, our system sets the ultrasound frequency at 40 kHz.

2.2 The Airborne Ultrasound Tactile Display with the Phased Array Scheme

The Airborne Ultrasound Tactile Display is a device which generates static pressure on the surface of objects with focused ultrasound [5][6]. Its upper surface is mounted with an array of ultrasound transducers attached in a lattice of 10 mm intervals. By adding proper phase shift on each transducer, the output ultrasound amplitude can be localized. Let r_i be the 3-dimensional position of the i-th transducer among N transducers and r_f be the desirable 3-dimensional (including the depth of the focus) focal position. The phase shift on each transducer θ_i is calculated so that it compensates the phase delay through distance:

$$\theta_i = k \left| r_i - r_f \right|.\qquad(2)$$

Here k denotes the wavenumber. Based on this phased-array scheme, a 2-cm-diameter spot of radiation pressure can be formed near the array. The spot can be moved in accuracy of 1mm horizontally. Its position can be switched at a refreshing rate of over 2 kHz. The whole phase calculation can be done in 50μs, which is faster than 2 kHz.

2.3 Waveform Calculation

The driving voltage signals of ultrasound transducers in our current setup are digital pulse waves. The transducers have a very sharp band-pass frequency characteristic of input voltage. As a result, the 40 kHz components in the input pulse voltage are derived as output ultrasound waveform. The amplitude of this 40 kHz component can be controlled by tuning the duty cycle of input pulse voltage. Suppose the frequency of the input pulse is set to 40 kHz and its duty cycle is set to d ($0 \leq d \leq 1/2$). The RMS of output ultrasound amplitude becomes

$$p = p_0 \sin(\pi d),\qquad(3)$$

where p_0 denotes the amplitude when d is equal to 1/2 [6]. Therefore, resulting waveforms can be controlled by changing the duty cycle of input voltage temporally. From (1) and (3), when the duty cycle is expressed as a time-variant function $d(t)$, the resulting radiation pressure can be expressed as

$$\begin{aligned} P(t) &= \frac{\alpha}{\rho c^2} p_0{}^2 \sin^2(\pi d(t)) \\ &= \frac{\alpha}{\rho c^2} p_0{}^2 \left[\frac{1 - \cos(2\pi d(t))}{2} \right]. \end{aligned}\qquad(4)$$
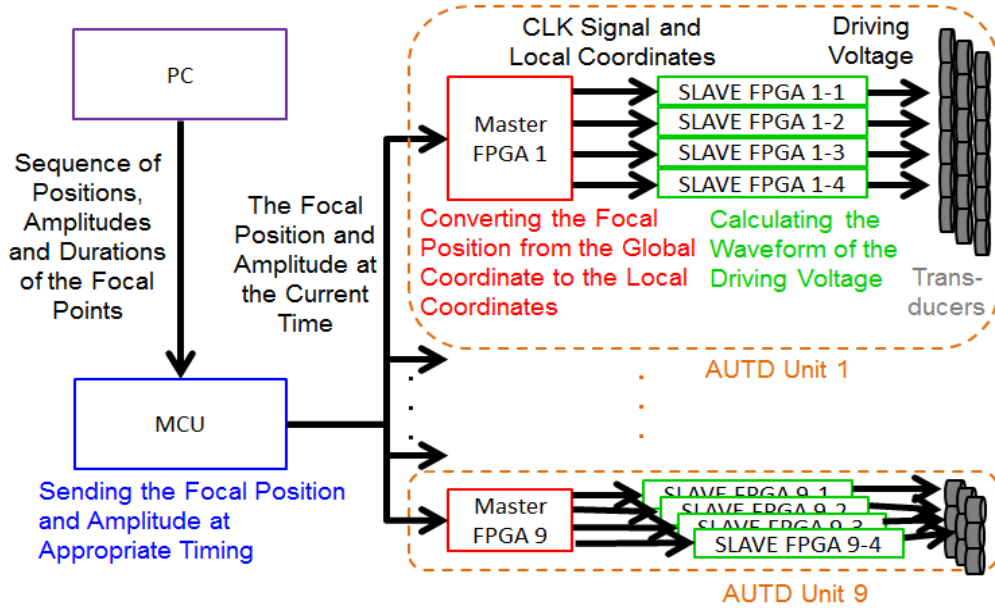
Figure 3: Diagram of system overview.

Using this relation, the driving pattern $d(t)$ for a given radiation pressure waveform $P(t)$ can be obtained as

$$d(t) = \frac{1}{2\pi}\cos^{-1}\left(1 - \frac{2\rho c^2}{\alpha p_0^2}P(t)\right). \qquad (5)$$

Since the value of cosine should be between -1 and 1, the term $\frac{2\rho c^2}{\alpha p_0^2}P(t)$ must not exceed 1. This term can be considered as a normalized output waveform of radiation pressure. The relation between these three function $d(t)$, $p(t)$ and $P(t)$ is depicted in figure 2. Due to the low-pass characteristics of human skin and mechanoreceptors, the squared envelope $P(t)$ is what we feel as vibrotactile sensations.

The given radiation pressure $P(t)$ can be generated from a recorded signal by resampling and rectifying the negative part of the signal.

3   SYSTEM CONSTRUCTION

In this paper we introduce our new vibrotactile display system fabricated using the AUTD scheme. Our first prototype [6] has almost the same scheme but implies some limitations. They are: 1) narrow workspace due to its small aperture (array size) and 2) coarse texture presentation due to its coarse amplitude quantization. We have overcome these issues and succeeded in focusing in further areas and producing various profiles of vibrotactile stimulation.

3.1   Large-Aperture Multi-Unit Phased Array Scheme

A phased array of ultrasound transducers plays a role as an ultrasound lens to produce a focal spot. Its focal point is variable as mentioned above. As a focusing performance of a lens highly depends on its aperture size, the array size of AUTD directly limits the depth range of proper focusing. In general, the spot blur size l is given as $l = A\frac{\sqrt{D^2+f^2}}{D}\lambda$ where A is the constant determined by the condition of image formation and D, f and λ

denotes the aperture length, the distance between the focal point and the AUTD surface, and the wavelength respectively. This equation indicates that the spot size remains comparative to the wavelength (diffraction limit) within the depth of the array diameter. This is the reason our previous prototype could only focus within approximately 20 cm close to the array.

To overcome this problem, we proposed the multi-unit scheme and performed some numerical simulations in our previous research [10]. As a result, it was confirmed that a wider aperture prevented the focusing in far field from being blurred. We constructed a 4-unit AUTD system subsequently, which could not perform well due to the inter-unit gaps that played a role as spatial filter and eventually the focusing was imperfect.

We reconstructed the new multi-unit system with a newer type of array units. They are fabricated so that the gap between units is 1cm. The signal transmission scheme between units has been replaced by the serial communication to reduce wiring.

Beside the improvement of spatial resolution of the pressure distribution in far field, output pressure is also magnified. The current system comprises 9 units and the number of transducers is 2,241 in all. As a result, the output radiation pressure at the focal point was expected to be approximately 400 Pa from the measurement. The gross force measured around the focal point reached 7.4 gf. Since the delay of signal transmission between AUTD units is around 50ns in the system, the implementation in this paper can easily be extended to a larger number of units to configure a larger aperture.

3.2   Finer Quantization of Output Amplitude

Since the output power was much improved, it became more realistic to create the variety of displayed vibrotactile sensation by tuning the temporal driving pattern appropriately. In particular, ultrasound envelope of a high sampling rate and a fine quantization is needed. In order to realize this, the driving pulse $d(t)$ has to vary quickly and its dynamic range has to be as wide as possible. Our current AUTD units include 25.6 MHz internal clocks and the driving pulse signals are generated from them. Thus the duty cycle of 40 kHz pulse $d(t)$ can be quantized up to
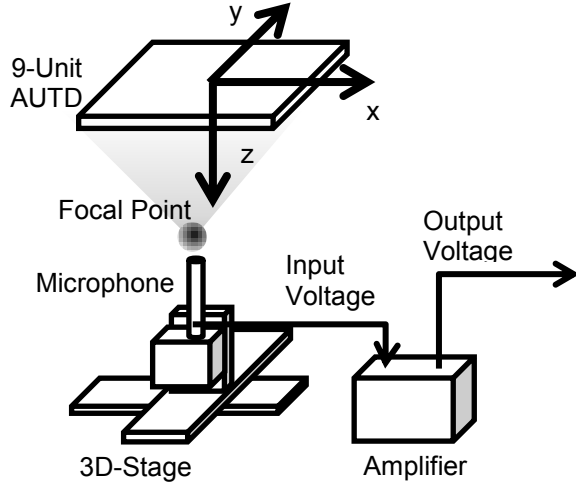
Figure 4: Diagram of the experimental setup of the pressure distribution measurement.

Figure 5: Two-dimensional radiation pressure distribution at z = 600mm.

Figure 6: One-dimensional radiation pressure distribution at y = 0 and z = 600mm.

640 levels. From (3) and (4), it is shown that the radiation pressure $P(t)$ is quantized up to 320 levels, which has been improved from 8 levels in the previous prototype. The current system can switch the duty cycle fast enough to generate vibrotactile sensation with the temporal resolution of 0.5 ms (2 kHz).

3.3 System Overview

Figure 3 depicts the diagram of system overview. The desired vibrotactile pattern to be generated is expressed as a temporal sequence of focal point data. Each datum s_i consists of a three-dimensional focal position (x_i, y_i, z_i), a focal amplitude p_i and a focal duration τ_i. A focal duration is the duration that the corresponding focal point is being produced. By giving an appropriate sequence of these parameters, the spatial and temporal profile of a focal point can be controlled as desired.

The sequence is sent to the Micro Controller Unit from PC via the serial communication. The MCU receives the focal point sequence and send the focal information of the current time to the Master FPGAs of all AUTD units via the serial communication. The timing is counted by an internal clock of the MCU. The focal information here includes the focal position(x, y, z) and the amplitude p. Each AUTD unit includes five FPGAs. One of them is for receiving the focal information from the MCU and we call it the Master FPGA. The rest four of them are the Slave FPGAs, which calculate the phase delays and generate all driving signals on transducers according to the focal position and the amplitude.

Each AUTD unit must know where it is in the global coordinates and its own posture as well. This information is at first sent to the Master FPGA of each AUTD unit. Since all the focal information sent is in the global coordinates, the Master FPGAs convert it to their own local coordinates, which the Slave FPGAs receive.

4 EXPERIMENTS

We operated experiments in order to verify that the temporal and spatial profile of the radiation pressure was generated in control. In the first experiment we confirmed how appropriately the 9-unit AUTD focused ultrasound at the distance of array size (60cm far from the AUT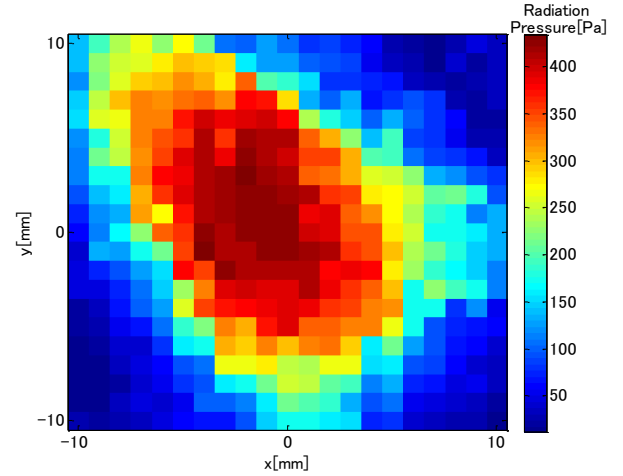D surface). The second experiment was performed for observing the output waveform of focused ultrasound and comparing it with the desired waveform. The wave sources were artificially generated. In addition, a subject study of a task to distinguish vibrotactile stimulation was performed.
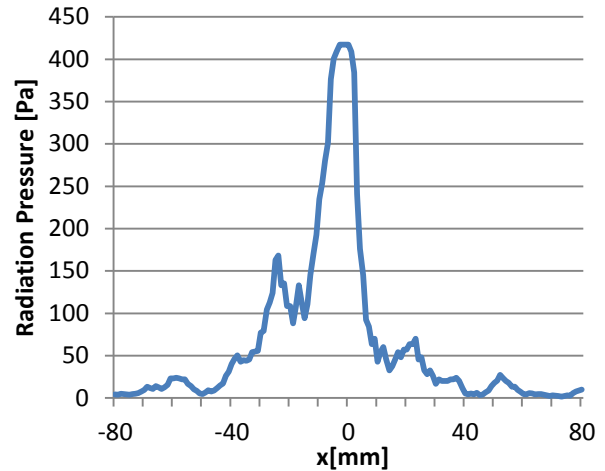
4.1 Pressure Distribution Measurement

We measured the spatial distribution of ultrasound amplitude in the experiment. Figure 4 shows the experimental setup. The 9-unit AUTD was mounted on an aluminum cabinet so that the transducer surface faced the ground. The surface was parallel to the ground. A standard microphone (Brüel&Kjær Type 4138) with a pre-amplifier (Brüel&Kjær Type 2670) was mounted on the 3D stage, whose xy-plane is parallel to the AUTD. The xy-coordinates corresponded with the lattice of transducers and the z-axis was vertical to the AUTD surface. The recorded voltage was amplified with a power amplifier (Brüel&Kjær Type 5935). We used the reference sound source which could provide 94dB sine wave of 1 kHz for the mapping of the recorded voltage to sound pressure. The frequency characteristic of the whole recording system was almost flat from 0 to 40 kHz. The array size was 576 mm x 454.2mm.
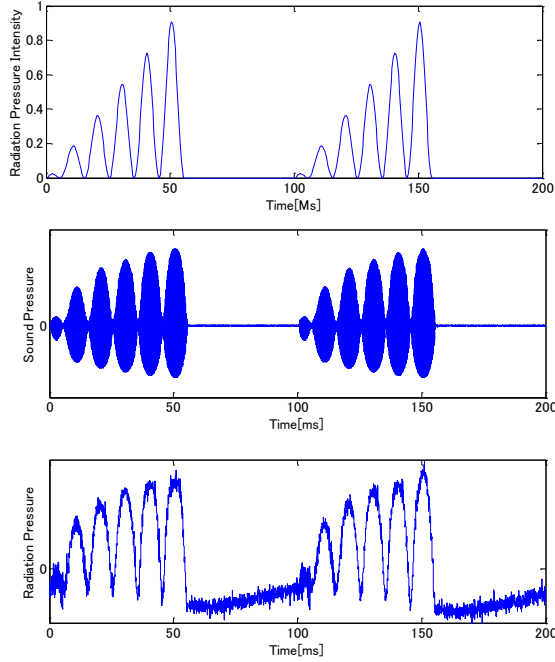
Figure 7: An example of input signal of radiation pressure (upper), generated sound pressure (middle) and radiation pressure (lower).

The focal point was set to (0, 0, 600mm). We measured sound pressure near the focal point and estimated the produced radiation pressure from eq.(1). The parameters were set as c=340m/s, ρ=1.18kg/m^3 and α=2. Figure 5 depicts the calculated radiation pressure distribution in 2d-plane at z = 600mm. High radiation pressure can be seen localized within the diameter of 10~15 mm. Also, the directivity of the pressure distribution can be seen due to the aperture of the AUTD was rectangular. A more macroscopic distribution is depicted in figure 6. This is a 1D distribution across the focal point where y and z were set to 0 and 600, respectively. The radiation pressure can be seen drastically attenuate outside of the focal regions.

4.2 Vibrotactile Sensation Identification

In this experiment we generated four different vibrotactile patterns and human subjects distinguished them only by touch. An example of recorded sound pressures and radiation pressures generated from an input waveform pattern is shown in figure 7. An Asymmetric sound pressure waveform, which caused radiation pressure, is seen in the figure. The radiation pressure amplitude is derived from the measured sound pressure amplitude by eliminating its 40 kHz or higher components. In the figure the generated radiation pressure has its temporal profile similar to the input signal.

Figure 8 shows the temporal profiles of the four vibrotactile patterns displayed on subjects' skins. The time integration of applied force generated from each pattern was adjusted to be equal so that the subjects would not be able to identify the displayed patterns by their average force intensity. A 100-Hz sine wave is modulated by each envelope in the pattern (iii: non-attenuating vibration) and (iv: attenuating vibration). The envelopes of the patterns (i: static pressure with impulsive rising and falling edges, like a mouse click) and (iii) are identical and the same goes for the patterns (ii: static pressure starting with rising edge and attenuating end) and (iv). We chose these patterns in order to assess how accurately subjects can distinguish 1) static
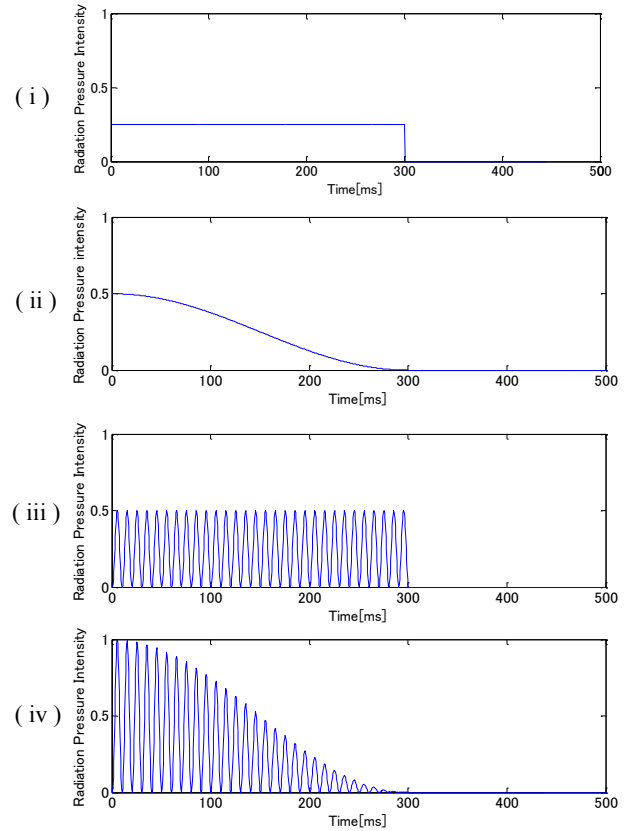

Figure 8: The four vibrotactile stimulation patterns added on subjects' skins.

and vibrating stimuli with the same envelope, and 2) envelopes of stimulation waveforms when the carrier waveforms are the same. The durations of all patterns were set to 300 ms, which we considered a typical duration of a mouse click.

Six subjects were asked to identify the vibrotactile stimulation which the AUTD generated on their palms among the four patterns described above. The stimulation was in a non-moving spot set to a time-invariant identical position. The distance between the subjects' palms and the AUTD was approximately 680 mm. The waveforms were printed on a piece of paper and the subjects were able to see it throughout the experiment. Before the identification task, the subjects received each stimulus pattern on their palm being informed of the stimulus number. Since the AUTD made characteristic noises when generating focused ultrasound, the subjects' wore headphones and heard white noises to mask those sounds during the task (figure 9). Throughout the experiment, no visual clue such as the obvious deformation of the skin surface was seen. The four patterns were displayed 10 times each, 40 times in all. The patterns were displayed repeatedly until the subject gave an answer. The sequence of the patterns was randomized. All subjects were male and their ages were between 22 and 47.

Figure 10 shows a graph of the correct answer ratios of the experiment. The error bars here indicates standard deviations of the correct answer ratios. The pattern (i) and (ii) were identified much more accurately than the rest of them. Some of the subjects claimed that the perception of the falling edges was a clue in distinguishing the pattern (i) from (ii). One of the other subject argued that he could feel the attenuation of the pressure in the pattern (ii), which became his clue for differentiation of the

Figure 9: Picture of the identification experiment.
On the top of the cabinet was the 9-unit AUTD mounted.

pattern (i) and (ii).

Table 1 shows a confusion matrix between the subjects' answers and actual displayed patterns. The number in the table indicated the numbers of times of answers. The table indicates that all subjects were able to differentiate the pattern (i) and (ii) from (iii) and (iv). It can be said that the differentiation between the pattern (i) and (ii) were easier than that between (iii) and (iv). Distinction between the falling edges of the envelope of (iii) and the attenuation pattern of (iv) felt vague.

5   Conclusion

A new remote vibrotactile display with a wide workspace was proposed and its performance was described in this paper. The proposed new AUTD system integrated multiple ultrasound transducer units and constructed an array of 576 mm x 454.2mm aperture. The new system succeeded in producing highly localized vibrotactile sensations on human skin 600 mm apart from the device. The focal intensity was experimentally demonstrated to be 7.4 gf. Temporal profiles of vibrotactile sensations were programmable with a sampling rate of 2 kHz and 320-level quantization. It was shown that typical examples of temporal force profiles in 300 ms duration were distinguishable for human subjects.

Our future work includes widening the spatial variety of the vibrotactile stimulation. Since it is possible for our system to reproduce the vibrotactile stimulation from real recorded signals, the pursuit of the reality of generated stimulation remains as another important issue.

References

[1] D.G. Caldwell, N.Tsagarakis and C.Giesler, "An integrated

Table 1: Confusion matrix between the subjects' answers
and actually displayed patterns.

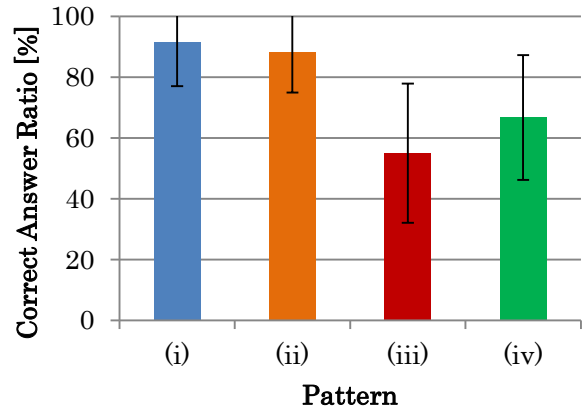| Answered / Displayed	(i)	(ii)	(iii)	(iv)
(i)	55	5	0	0
(ii)	7	53	0	0
(iii)	0	0	33	27
(iv)	0	0	20	40

Figure 10: The correct answer ratio.

tactile/shear feedback array for stimulation of finger mechanoreceptor," Proc. of IEEE International Conference on Robotics and Automation, vol.1, pp.287-292, 1999.

[2] S. Tsuchiya, M.Konyo, H.Yamada, T.Yamauchi, S.Okamoto and S.Tadokoro, "VibTouch: Virtual Active Touch Interface for Handheld Devices," Proc. of 18th IEEE International Symposium on Robot and Human Interactive Communication, pp.12-17, 2009.

[3] J. C. Gwilliam, A. Degirmenci, M. Bianchi and A. M. Okamura, "Design and Control of an Air-Jet Lump Display," IEEE Haptics Symposium, pp. 45-49, 2012.

[4] R. W. Lindeman, Y. Yanagida, H. Noma and K. Hosaka, "Wearable Vibrotactile Systems for Virtual Contact and Information Display," Virtual Reality, Vol.9, pp. 203-213, 2006.

[5] T. Iwamoto, M. Tatezono and H. Shinoda, "Non-contact method for producing tactile sensation using airborne ultrasound," Proc. of EuroHaptics 2008, pp. 504-513, 2008.

[6] T. Hoshi, M. Takahashi, T. Iwamoto and H. Shinoda, "Noncontact Tactile Display Based on Radiation Pressure of Airborne Ultrasound," IEEE Transactions on Haptics, vol. 3, pp. 155-165, 2010.

[7] K. Minamizawa, M. Nakatani, Y. Kakehi, S. Mihara and S. Tachi, "TECHTILE Toolkit," in IEEE Haptics Symposium 2012, Demo, 2012.

[8] J. Awatani, "Studies on Acoustic Radiation Pressure. I(General Considerations)," Journal of the Acoustical Society of America, Vol. 27, pp. 278-281, 1955.

[9] P. J. J. Lamoreet, H. Muijser and C. J. Keemink, "Envelope detection of amplitude-modulated high-frequency sinusoidal signals by skin mechanoreceptors," Journal of the Acoustical Society of America, Vol. 79, pp. 1082-1085, 1986.

[10] M. Takahashi and H. Shinoda, "Large Aperture Airborne Ultrasound Tactile Display Using Distributed Array Units," Proc. of SICE Annual Conference, pp. 359-362, 2010.